Science of the Total Environment 666 (2019) 828–838

Contents lists available at ScienceDirect

Science of the Total Environment

journal homepage: www.elsevier.com/locate/scitotenv

Mercury bioaccumulation in tilefish from the northeastern Gulf of Mexico 2 years after the *Deepwater Horizon* oil spill: Insights from Hg, C, N and S stable isotopes

Vincent Perrot [a,*], William M. Landing [b], R. Dean Grubbs [c], Vincent J.M. Salters [a]

[a] National High Magnetic Field Laboratory, Florida State University, 1800 East Paul Dirac Drive, Tallahassee, FL 32310, USA
[b] Department of Earth, Ocean, and Atmospheric Science, Florida State University, 117 N. Woodward Ave, Tallahassee, FL 32306, USA
[c] Coastal and Marine Laboratory, Florida State University, 3618 Coastal Highway 98, St. Teresa, FL 32358-2702, USA

HIGHLIGHTS

- [Hg] in fish of the Gulf of the Mexico is a concern due to commercial fisheries.
- We hypothesized that the *Deepwater Horizon* oil spill affected Hg availability.
- About 90% of tilefish surpassed Hg thresholds of U.S. regulations for food.
- Mississippi River inputs combined with oil caused reduced Hg bioavailability.
- Hg concentrations and isotopes in fish organs reflect in vivo processes.

GRAPHICAL ABSTRACT

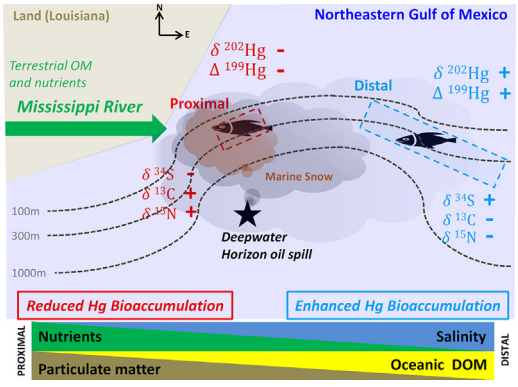

ARTICLE INFO

Article history:
Received 30 November 2018
Received in revised form 18 February 2019
Accepted 18 February 2019
Available online 20 February 2019

Keywords:
Methylmercury accumulation
Hg bioavailability
Natural stable isotopes
Mississippi River

ABSTRACT

Mercury (Hg) concentration in fish of the Gulf of the Mexico (GoM) is a major concern due to the importance of the GoM for U.S. fisheries. The *Deepwater Horizon* (DWH) oil spill in April 2010 in the northern GoM resulted in large amounts of oil and dispersant released to the water column, which potentially modified Hg bioaccumulation patterns in affected areas. We measured Hg species (methylmercury (MMHg) and inorganic Hg (IHg)) concentrations, and light (C, N and S) and Hg stable isotopes in muscle and liver tissues from tilefish (*Lopholatilus chamaleonticeps*) sampled in 2012 and 2013 along the shelf break of the northeastern GoM. Fish located close to the mouth of the Mississippi River (MR) and northwest of the DWH well-head (47 km) showed significantly lower Hg levels in muscle and liver than fish located further northeast of the DWH (>109 km), where 98% of tilefish had Hg levels in the muscle above US consumption advisory thresholds (50% for tilefish close to the DWH). Differences in light and Hg stable isotopes signatures were observed between these two areas, showing higher $\delta^{15}N$, and lower $\delta^{202}Hg$, $\Delta^{199}Hg$ and $\delta^{34}S$ in fish close to the DWH/MR. This suggests that suspended particles from the MR reduces Hg bioavailability at the base of the GoM food chains. This phenomenon can be locally enhanced by the DWH that resulted in increased particles in the water column as evidenced by the marine snow layer in the sediments. On the other hand, freshly deposited Hg associated with organic matter in more oligotrophic marine waters enhanced Hg bioaccumulation in local food webs. Comparing Hg isotopic composition

* Corresponding author at: Institut des Sciences de la Terre, Université Grenoble Alpes, 1381 Rue de la Piscine, Gières 38610, France.
E-mail address: vincent.perrot1@univ-grenoble-alpes.fr (V. Perrot).

https://doi.org/10.1016/j.scitotenv.2019.02.295
0048-9697/

in liver and muscle of fish indicates specific metabolic response in fish having accumulated high levels of MMHg.

1. Introduction

Several years after the catastrophic event of the *Deepwater Horizon* (DWH) oil spill in the northern Gulf of Mexico (nGoM) in April 2010, little is known about the real extent of the consequences in terms of ecological impact on GoM ecosystems (Coelho et al., 2013; Paul et al., 2013; Prince and Parkerton, 2014). Both field and experimental studies show that the oil spill severely affected the development and function of several essential organs in fish (Brette et al., 2014; Dubansky et al., 2013; Incardona et al., 2014). It is not well documented, however, if the DWH event had long term effects (direct or indirect) on wildlife response to other chronic contaminations such as toxic trace metals. Mercury (Hg) bioaccumulation in fish is a major concern in the GoM, since its waters produce nearly 20% of US commercial and 40% of recreational fisheries landings (NMFS, 2017; NOAA, 2011).

Elevated concentrations of methylmercury (MMHg), a subtle neurotoxin, in several fish species of the northern GoM have been reported for decades (Adams et al., 2003; Cai et al., 2007), leading to the establishment of fish consumption advisories in order to reduce the risk of exposure to humans. The Hg cycle in marine waters is complex and strongly depends on physical, ambient chemical, and microbiological conditions that affect Hg bioaccumulation in food webs (Fitzgerald et al., 2007). Microbial communities, such as sulphate-reducers (SRBs), are known for being major players for MMHg production and degradation in the water column or at the sediment/water interface (Bridou et al., 2011; Compeau and Bartha, 1985; Parks et al., 2013). During the DWH event, oil was released from an oil well for several months in a large plume in the water column, and a component was deposited on the surrounding seafloor and coastal zones (Chanton et al., 2015; Liu et al., 2011; MacDonald et al., 2015; Mendelssohn et al., 2012; Poje et al., 2014). While the oil should not have directly impacted the Hg concentrations in the GoM waters due to low Hg concentration in the oil (Wilhelm et al., 2007) and subsequent dilution in the water column, the DWH had locally a significant impact on the sedimentation rates, microbial activity (such as SRBs, (Joye et al., 2014; Kleindienst et al., 2015; Lu et al., 2012)), and chemistry of the GoM waters and seafloor (Daly et al., 2016; Dubinsky et al., 2013; Hastings et al., 2016; Joye et al., 2014; Lu et al., 2012; Passow et al., 2012; Paul et al., 2013; Reddy et al., 2012; Spier et al., 2013). This might have led to changes in molecular Hg species production/degradation rates in the water column and the seafloor. It was also suggested that the DWH could have enhanced Hg evasion from the seawater to the atmosphere (Walsh et al., 2015), as it has been observed during another oil spill event (Pandey et al., 2009). The DWH and the added dispersants might also have modified, through fish health perturbations (Ainsworth et al., 2018; Brette et al., 2014; Incardona et al., 2014; Jung et al., 2009; Mager et al., 2014; Wise et al., 2014), the Hg accumulation and metabolism in fish.

Mercury compounds are also sensitive to changes in water chemistry such as salinity, light intensity, and particulate and organic matter (Barkay et al., 1997; Black et al., 2012; Ravichandran, 2004; Schartup et al., 2015). The Mississippi River (MR), carrying 41% of U.S. riverine waters to the GoM, is a significant source of terrestrial material to the GoM supplying particulate and dissolved matter (nutrients, organic carbon, pollutants) (Cardona et al., 2016; Dagg et al., 2008; Rebich et al., 2011), which has strong implications for coastal biogeochemistry close to the Mississippi delta (Dagg and Breed, 2003; Rabalais et al., 2002; Swarzenski et al., 2008; Wang et al., 2004). Hence, in the coastal/inner shelf areas of Louisiana the production, degradation, and biological uptake of Hg compounds are likely to be affected by the MR plume. The MR has also been identified as a significant source of Hg to the GoM in addition to direct atmospheric deposition (Harris et al., 2012; Rice et al., 2009). Since the DWH well-head is located near (~80 km SW) the MR mouth, the Mississippi plume and the DWH plume were suggested to interact on the coastal shelf near the Mississippi mouth (Daly et al., 2016), which could affect local to regional Hg biogeochemistry in the northeastern continental shelves (Louisiana, Alabama and Florida shelves) of the GoM.

Light stable isotopes of carbon, nitrogen and sulphur are known to be powerful proxies for characterizing aquatic food webs (food sources, trophic status, feeding strategies, etc. (Carr et al., 2017; Post, 2002)), and combining Hg stable isotopes studies can help understand Hg processing in such environments (Blum et al., 2013; Perrot et al., 2012; Senn et al., 2010). Hg has seven naturally occurring stable isotopes that can be fractionated during natural transformations of Hg species (elemental Hg(0), inorganic Hg(II) and MMHg) (Bergquist and Blum, 2007; Kritee et al., 2013; Rodriguez-Gonzalez et al., 2009), where both mass-dependent fractionation (MDF) and mass-independent fractionation (MIF) can occur, depending on the nature of the transformation. Natural Hg isotopic variations measured in environmental samples are hence a result of one or several Hg sources with different isotope composition, and are also the fingerprint of several Hg transformations (methylation, reduction, etc.), before Hg was stored in the sample (e.g. review (Blum et al., 2014)). In the GoM, recent works showed that disconnected coastal and oceanic fish species displayed specific Hg isotopes signatures that highlighted different Hg cycling and potentially different Hg sources between coastal and off-shore fish (Kwon et al., 2013; Senn et al., 2010). In addition, while it seems likely that mammals are able to fractionate Hg isotopes in-vivo (Perrot et al., 2016; Perrot et al., 2012; Sherman et al., 2013), it is still under debate if processes such as trophic transfer, metabolization, detoxification, and/or excretion can significantly fractionate Hg isotopes in fish (Das et al., 2009; Kwon et al., 2012; Kwon et al., 2013).

We measured MMHg and inorganic (IHg) concentrations, as well as stable isotopic compositions of Hg and light isotopes (C, N, S), in muscle and liver of tilefish (*Lopholatilus chamaeleonticeps*) collected in the nGoM at different distances from the DWH blowout during two field campaigns in 2012 and 2013. Tilefish are demersal species that are found at depth between 100 and 400 m and are endemic to the western Atlantic Ocean including the Gulf of Mexico. They have relatively high site fidelity, live in burrows in sediments of the outer-continental shelf, shelf break and upper slope, and feed mostly on invertebrates (Jones et al., 1989; NOAA, 1999). Annually, 100–130 tons of tilefish are landed in a commercial longline fishery in the eastern Gulf of Mexico. Though the most recent stock assessment suggests tilefish are not overfished in the Gulf of Mexico, the species is assessed as *Endangered* in the IUCN Red List of Threatened Species due to long-term and continuous declines in Atlantic waters of the U.S. and Canada (Aiken et al., 2015). Tilefish have also been documented as a fish species of the GoM accumulating the highest amounts of Hg throughout their lifespan (Karimi et al., 2012); however, NOAA Fisheries lists tilefish as a smart seafood choice due to sustainable management with no mention of mercury concerns (https://www.fisheries.noaa.gov/species/tilefish). Interestingly, a study reported Hg concentrations (and other contaminants) in tilefish after the DWH in the northeastern GoM were lower than expected, but no fish were sampled in the near vicinity (i.e.

<100 km) of the DWH blow out site (Fitzgerald and Gohlke, 2014). Hence, the aim of this study was to investigate and compare Hg bioaccumulation in tilefish in an area close to the DWH and the MR mouth with more distal stations along the shelf break of the northern GoM.

2. Materials and methods

2.1. Sample collection and preparation

Tilefish samples were collected using fishery-independent longline surveys on the research vessels Weatherbird II and Apalachee in April, July and October 2012, and July and October 2013. Detailed survey methods are reported in (Churchill et al., 2015). Tilefish were sampled at 7 locations in the northern GoM (Fig. 1) ranging from 47 to 223 km away from to DWH well head site (Table S1). In order to allow a better comparison between the different sampling sites, fish samples were chosen if possible to be of similar size range at all sites (Table 1 and Fig. S1a). Fish standard length ranged from 37 to 76 cm (mean 50 ± 10 cm) and weight ranged from 0.9 to 10.0 kg (mean 2.7 ± 1.9 kg). Depending on the sampling station, fish were collected at depths between 204 and 337 m. A total of 62 muscle samples were selected for Hg-species (MMHg and IHg) concentrations analyses. When possible, a liver sample was also collected from the same fish for Hg compounds analysis. We obtained a total of 17 liver samples for our study because the other liver samples were used in other toxicological studies.

After sampling, fish organs were separated onboard, individually placed in Ziploc bags and frozen at −20 °C. Once at the laboratory, samples were stored at −18 °C until they were weighed then freeze-dried for 48 h. Samples were weighed again (wet weight/dry weight ratio = 4.7 ± 0.5), then ground to fine powder in an agate mortar. Freeze-dried and ground samples were finally stored in a freezer (−18 °C) until analysis.

2.2. Hg species concentration in tissues

A mass of 0.1–0.2 g of freeze-dried tissue was weighted in a 20 mL acid-cleaned glass vial, to which was added 5 mL of ultra-pure (distilled at the laboratory) 6 M HNO_3. Vials were sealed and put in an oven at 70 °C for 6 h for Hg species (MMHg and IHg) extraction. Vials were allowed to cool down and then stored in at 6–7 °C until analyses. Samples were then centrifuged and the supernatant was recovered. Hg species concentrations were measured using Tekran®2700 Mercury Analysis System. Briefly, the extract was diluted 3 times with ultrapure deionized water and a volume of 0.010 to 0.100 mL of this solution was derivatized in a 30 mL aqueous solution at pH 4.5 after adding 0.030 mL of 1% Sodium tetraethylborate as a derivatizing agent and subsequent hand shaking. Depending on the sample, from 0.5 to 30 ng L^{-1} of MMHg and IHg was derivatized. Then, the solution was purged into the Tekran®2700 system, where the ethylated IHg and MMHg species were trapped on a Tenax trap then desorbed and flushed to a Gas Chromatography oven in a capillary column where they were separated, and finally pyrolyzed and detected via atomic fluorescence spectrometry. The instrument was calibrated with solutions containing known MMHg and IHg concentrations (using MMHg and IHg standards solutions of 10 and 500 ng L^{-1}) in the range of 0 to 32 ng L^{-1}. Certified reference materials for MMHg and total Hg (Tuna muscle ERM-CE 464 and Dogfish liver NRCC DOLT-4) were measured periodically between tilefish samples to ensure the accuracy of the analysis. Duplicates of extractions, duplicates of derivatization as well as samples spiked with MMHg and IHg standards were also analyzed periodically to ensure the robustness of the method. The precision of the method, as relative standard deviation, was typically better than 5%. Limit of quantification was typically lower than 0.05 ng L^{-1} for MMHg and lower than 0.2 ng L^{-1} for IHg. Hg species concentrations are reported as μg Hg g^{-1} muscle on a dry weight basis.

2.3. Hg stable isotope ratios analysis

A mass of approximately 0.2 g of dry weight tissue was weighted in a 20 mL acid-cleaned glass vial, to which were added 4 and 1 mL concentrated and ultra-pure HNO_3 and HCl, respectively. Vials were loosely capped for 1 h, then sealed and left overnight at room temperature. Then 4 mL of deionized water was added and vials were heated at 80 °C on a hot-plate for 4 h (1.5 h of ramp and 2.5 h of heating time). After the samples were cooled, 0.8 mL of BrCl was added to ensure complete oxidation of Hg to Hg(II). Samples were then centrifuged and the supernatants were recovered and stored in glass vials. An aliquot of the supernatant was pipetted and diluted to reach 2 μg L^{-1} in 5% acid (HNO_3, HCl, BrCl) in a total volume of 10 mL, assuming total Hg concentration of a fish sample to be the sum of MMHg and IHg concentrations measured by Tekran® 2700. Just prior to analysis 0.3 mL of 0.72 M hydroxylamine (NH_2-HCl)

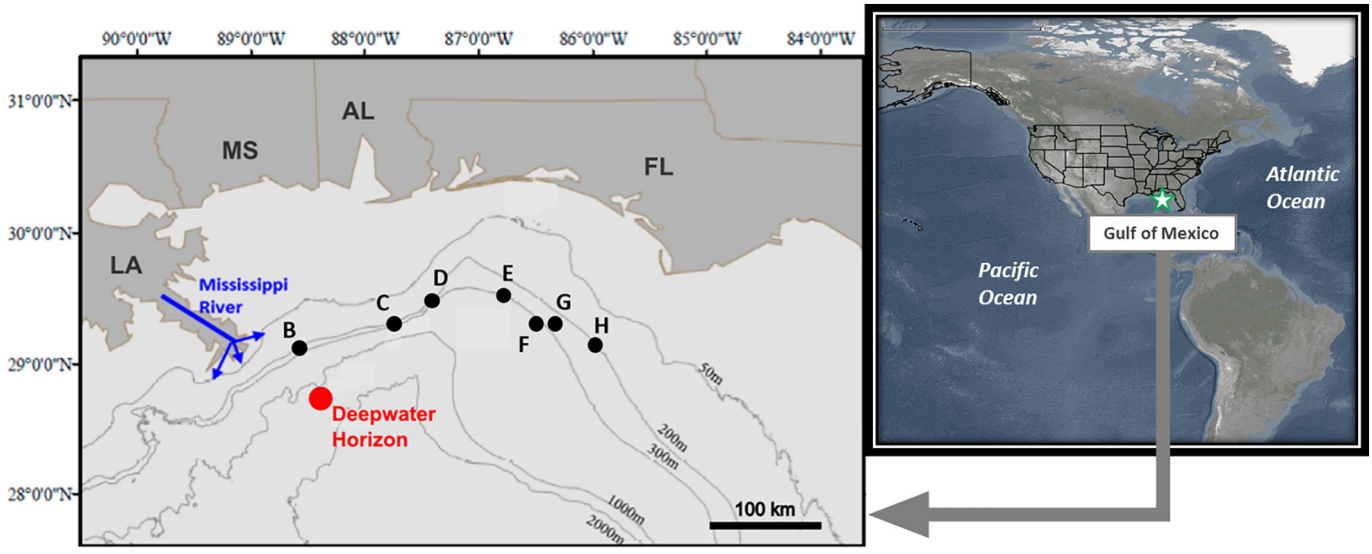

Fig. 1. Sampling sites of Tilefish in the northern Gulf of Mexico. Seven different sampling stations were located from 47 to 223 km away from the DWH well: B, 47 km; C, 85 km; D, 109 km; E, 124 km; F, 192 km,; G, 207 km,; H, 223 km. The well head of the DWH is located 28.738 N, 88.366 W. Latitude and longitude of each site are given in Table S1.

Table 1
Average values and associated standard deviation for Hg species in fish muscle and fish size for each sampling station.

Station code	n	Std length (cm)	Body weight (kg)	[MMHg] (μg g^{-1} dw)	[IHg] (μg g^{-1} dw)	[THg] (μg g^{-1} dw)	% MMHg	[THg]/weight	[THg]/length
B	10	57 ± 12	4.1 ± 2.9	1.52 ± 0.81	0.04 ± 0.02	1.57 ± 0.85	97 ± 1	0.5 ± 0.3	0.03 ± 0.01
C	1	48	1.9	0.89	0.02	0.90	98	0.5	0.02
D	17	49 ± 9	2.7 ± 1.6	4.09 ± 2.04	0.10 ± 0.05	4.19 ± 2.10	97 ± 1	1.8 ± 0.8	0.08 ± 0.04
E	16	49 ± 9	2.3 ± 1.5	3.97 ± 1.15	0.08 ± 0.03	4.06 ± 1.17	98 ± 1	2.3 ± 1.2	0.08 ± 0.02
F	9	52 ± 9	2.9 ± 2.0	4.32 ± 2.15	0.09 ± 0.07	4.41 ± 2.21	98 ± 1	1.8 ± 0.8	0.08 ± 0.03
G	3	44 ± 9	1.8 ± 1.5	2.55 ± 1.23	0.06 ± 0.04	2.61 ± 1.27	98 ± 1	1.8 ± 0.8	0.06 ± 0.02
H	6	47 ± 7	1.9 ± 1.1	3.58 ± 1.07	0.09 ± 0.05	3.66 ± 1.12	98 ± 1	2.0 ± 0.7	0.08 ± 0.02

was added to the sample to remove the excess of BrCl. For Hg isotope ratios (IRs) analysis, the sample was introduced in a multi-collector ICP-MS (ThermoFinningan® Neptune) using a cold vapor generator (CETAC® HGX-200) as an introduction system. Briefly, Hg(II) in samples was reduced on-line with 3% $SnCl_2$ in 5% HCl prepared daily and introduced into the instrument as elemental Hg in an Argon stream. The bracketing standard method was used to report the per mil (‰) deviation of the samples versus Hg international standard NIST 3133. Each measurement of sample IRs was preceded and followed by the measurement of Hg NIST 3133 IRs at a concentration of 2 μg L^{-1} and prepared in the same acidic matrix than the sample. The isotopic composition of the sample was reported as delta values (δ) for 5 Hg isotopes (199, 200, 201, 202, 204) versus isotope 198 (Blum and Bergquist, 2007):

$$\delta^{xxx}\mathrm{Hg} = \left(\left(\left({}^{xxx}\mathrm{Hg}/{}^{198}\mathrm{Hg}\right)_{sample}/\left({}^{xxx}\mathrm{Hg}/{}^{198}\mathrm{Hg}\right)_{NIST3133}\right)-1\right) \times 1000 \quad (1)$$

δ^{202} Hg is used as the signature of the MDF of Hg isotopes in fish tissues in this manuscript. To report the MIF of Hg isotopes, capital delta values (Δ) represent the deviation from the theoretical MDF for each Hg isotope:

$$\Delta^{xxx}\mathrm{Hg} = \delta^{xxx}\mathrm{Hg} - \left(\delta^{202}\mathrm{Hg} \times \beta\right) \quad (2)$$

where β is 0.2520, 0.5024, 0.7520, and 1.4930 for isotope 199, 200, 201 and 204 respectively. Secondary Hg standard UM-Almaden, prepared at 2 ng/mL in the same matrix as samples and NIST3133, was periodically analyzed for Hg IRs about once every 6 samples, and was used to report the accuracy and the precision of the method. A total of 38 measurements of Hg UM-Almaden were performed during different sessions of analysis. Average UM-Almaden isotopic composition was in agreement with previously published values (Blum and Bergquist, 2007) with δ^{202} Hg, Δ^{199} Hg and Δ^{200}Hg of −0.58 ± 0.16, −0.02 ± 0.08 and 0.01 ± 0.12 (‰, 2SD), respectively.

2.4. Light stable isotopes analysis

Twenty-three samples of tilefish muscle were selected among different sampling stations for light stable isotopes ratios analysis of carbon, nitrogen and sulphur. Isotopic ratios are reported as delta values for C (δ^{13}C), N (δ^{15}N) and S (δ^{34}S) that are the deviation (‰) of the sample relative to an international standard, i.e. Vienna Pee Dee Belemnite, atmospheric nitrogen and Vienna Cañon Diablo Trolite for C, N and S, respectively. Carbon and Nitrogen isotopic ratios were measured in our laboratory, using a Thermo Fischer Scientific Delta Plus XP Isotope Ratio Mass Spectrometer coupled with a ThermoQuest CE Instrument NC2500 Elemental Analyzer and a Thermo Fisher Scientific Conflo III. Sulphur isotopic ratios were measured at the Stable isotope Core Laboratory (Washington State University, WA) using a continuous flow isotope mass spectrometer (DeltaPlusXP, Thermofinnigan) coupled with an elemental analyzer (ECS 4010, Costech Analytical) (Brenna et al., 1997). Typical standard deviation was 0.12, 0.18 and 0.20 for δ^{13}C, δ^{15}N and δ^{34}S, respectively.

2.5. Data analysis

All data and figures were analyzed and created with Microsoft Office Excel® software, using Data Analysis Tool Box for statistics (*t*-test assuming unequal variances and $\alpha = 0.05$, and regressions with a confidence level of 95%).

3. Results and discussion

3.1. Hg concentration in tilefish tissues

3.1.1. Hg in muscle

Overall, total Hg (THg) in tilefish muscle averaged 3.59 ± 1.87 μg g^{-1} (1SD, $n = 62$; range 0.71–9.42 μg g^{-1}) and increased with fish weight (Fig. 2) and length (Fig. S1b). Methylmercury represented 97.7 ± 0.8% of THg, with concentrations increasing linearly with THg (Fig. S2a). Significant differences were observed among and between the different stations (Table 1, Fig. 2, Fig. S1b and Table S2). Tilefish sampled at stations B and C, the closest to the DWH site, showed the lowest concentrations of Hg in their muscle with MMHg averaging 1.52 ± 0.82 μg g^{-1} (range 0.70–3.33, $n = 10$) and 0.89 μg g^{-1} (n = 1), respectively. Sampling station C will not be discussed further since only one fish was sampled there. Conversely, tilefish caught farther than 109 km away from the DWH site, i.e. stations D, E, F, G, and H, showed the highest MMHg concentrations in their muscle with MMHg averaging 4.09 ± 2.04 μg g^{-1} (range 1.39–7.97, $n = 17$), 3.97 ± 1.15 μg g^{-1} (range 2.08–6.19, $n = 16$), 4.32 ± 2.15 μg g^{-1} (range 2.63–9.18, $n = 9$), 2.55 ± 1.23 μg g^{-1} (range 1.41–3.86, $n = 3$) and 3.58 ± 1.07 μg g^{-1}

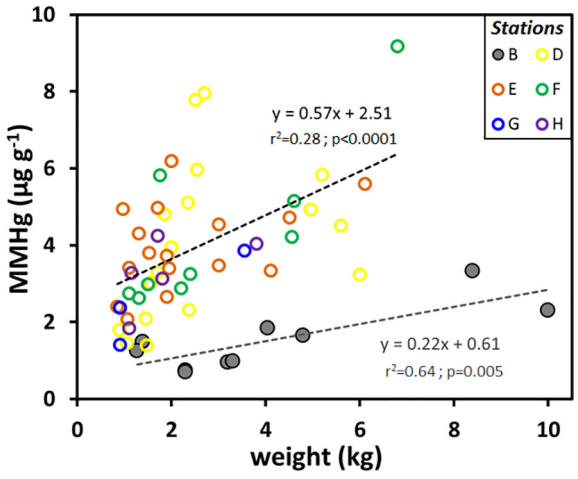

Fig. 2. MMHg concentrations in muscle as a function of fish weight for 61 tilefish caught at different locations in the northern GoM.

(range 1.84–4.92, n = 6), respectively. Those significant differences cannot be attributed to difference in length or weight (Fig. 2 and Fig. S1b), as also shown by normalisation of THg in the muscle versus the weight and the length of the fish (Table 1 and Table S2). For all sampling stations, fish showed a decrease of THg/weight with increasing weight (Fig. S1c). Fish caught at station B averaged THg/weight ratio of 0.5 ± 0.3 and THg/length ratio of 0.03 ± 0.01 (n = 10). Those ratios are almost one order of magnitude lower than the average THg/weight and THg/length ratios for stations D, E, F, G, and H taken together (1.96 ± 0.92 and 0.083 ± 0.030 (n = 51), respectively). Significantly higher THg/weight ratios were observed in 2012 compared to 2013 for sampling stations far from the DWH (>109 km), whereas no significant differences were observed close to DWH (Fig. S3). Overall, about 90% of the tilefish caught for this study (56 out of 61) displayed Hg concentrations in the muscle that are above the U.S. EPA recommendation value for daily consumption (0.3 μg g^{-1}, wet weight). For tilefish close to the DWH, 50% (5 out of 10) were below this value, whereas far from the DWH only 2% (1 out of 51) were below this value.

3.1.2. Hg in liver

Total Hg in liver averaged 4.00 ± 3.40 μg g^{-1} (1SD, n = 17; range 0.68–12.5 μg g^{-1}), and IHg dominated Hg speciation (80 ± 13% of IHg, range 61–98%) (Table S3), and increased linearly with THg (Fig. S2b). As for muscle, liver of the single tilefish from station B contained significantly lower THg (1.85 μg g^{-1}) than those from stations D, E, F, G, and H (average 4.14 ± 3.46 μg g^{-1}, n = 16). This is strengthened when comparing the THg/weight ratio in the liver of this fish (0.39) with fish with similar weight (4 to 5 kg) from other stations (1.07 ± 0.21, n = 4). Among tilefish far from DWH, one fish (DC-13-502, station H)that contained the highest THg amount in the liver (12.5 μg g^{-1}), displayed a significantly higher ratio $IHg_{liver}/MMHg_{muscle}$ (2.1) compared to other samples (average 0.9 ± 0.4, n = 16). This high ratio can be compared to a study which reports higher $THg_{liver/muscle}$ ratios in Hg contaminated freshwater compared to uncontaminated sites (Havelkova et al., 2008). However, no local Hg contamination source is expected here. Despite differences in %IHg in liver among samples, IHg is the dominant species in livers (Fig. S2b), as opposed to the muscle samples where MMHg drives THg concentrations (Fig. S2a). THg values in the liver were correlated with THg in the muscle (Fig. 3a), and IHg concentrations in the liver were also positively correlated to the MMHg levels in the muscle (Fig. 3b). These observations support the theory of in vivo demethylation in fish (Khan and Wang, 2010; Wang et al., 2013; Yamashita et al., 2013), where the MMHg accumulated in the muscle is related to the IHg stored in the liver, the latter being the product of a fraction of the MMHg that is degraded and then stored in the liver. However, two recent studies suggest that in vivo MMHg demethylation in marine fish occurs in the intestine rather than in the liver (Wang et al., 2017; Wang and Wang, 2017).

3.2. Stable isotopic composition of tilefish tissues

3.2.1. Light stable isotopes

Nitrogen, carbon, and sulphur isotope analysis were performed using muscle samples from 23 tilefish: $\delta^{15}N$ averaged 13.6 ± 0.8‰ and ranged from 11.9 to 14.9‰ (about 1 trophic level unit range (Post, 2002)); $\delta^{13}C$ averaged −17.3 ± 0.4‰ and ranged from −16.5 to −18.3‰; $\delta^{34}S$ averaged 19.9 ± 1.2‰ and ranged from 17.8 to 21.2‰ (Table S4 and Fig. S5). Fig. S5a shows that $\delta^{13}C$ and $\delta^{15}N$ were positively correlated at both station B and other stations, while $\delta^{13}C$ vs. $\delta^{34}S$ and $\delta^{15}N$ vs. $\delta^{34}S$ showed negative correlations only for station B (Fig. S5b and c), i.e. $\delta^{13}C$ and $\delta^{15}N$ increased with decreasing $\delta^{34}S$. No significant differences were observed between station B and stations >109 km from DWH for $\delta^{13}C$ (−17.1 ± 0.4 and −17.5 ± 0.4‰, respectively, t-value = 1.94, p-value = 0.07), indicating similar carbon source and same basal resources associated with benthic production (Thomas and Cahoon, 1993). On the other hand, $\delta^{15}N$ values of tilefish caught close to station B were significantly higher (t-value = 3.35, p-value = 0.003) than those of tilefish caught farther from DWH (stations D, E, F, G) (14.2 ± 0.5‰ and 13.2 ± 0.7‰, respectively). This indicates, for example, that tilefish from station B either feed at a higher trophic level due to change in diet after the DWH oil spill (Tarnecki and Patterson III, 2015), have higher $\delta^{15}N$ at the base of their food chain (Cabana and Rasmussen, 1996; Post, 2002), or simply have different diet than tilefish located >109 km from DWH. We also observed significant differences (t-value = −6.37, p-value<0.00001) for $\delta^{34}S$ between fish from station B and fish from other stations, with fish located close to the DWH and the mouth of the MR having a lower mean value (18.6 ± 1.0‰) than fish from stations farther from the MR mouth (20.6 ± 0.5‰). This result can be attributed to the larger influence of freshwater discharge from the MR (Morey et al., 2003) for station B than for other stations that have S isotopic signature closer to sulphate seawater (~21‰, (Rees et al., 1978)). Stimulation of bacterial sulphate-reduction activity at stations close to DWH by the released oil and/or dispersants (Kleindienst et al., 2015) may also contribute to the lighter sulphur isotopic composition measured in fish close to the well-head due to S isotopic fractionation during sulphate-reduction by SRB (Kleikemper et al., 2003; Pellerin et al., 2015; Sim et al., 2011).

Positive correlations were observed between $\delta^{15}N$ and MMHg, and between $\delta^{13}C$ and MMHg in tilefish from stations D to G, but not at station B (Fig. S6). This indicates increasing Hg accumulation with trophic level at more eastern stations, but not close to the at MR-DWH stations. Higher MMHg concentrations together with lower $\delta^{15}N$ at eastern

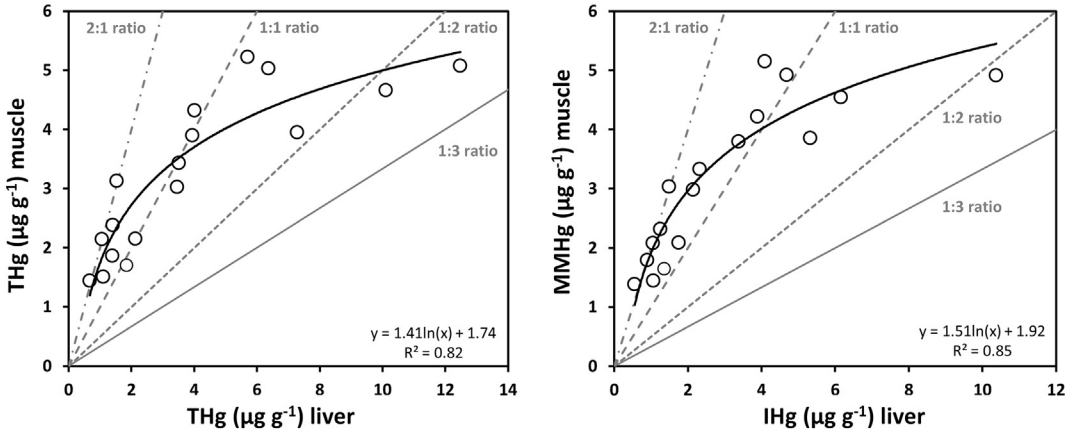

Fig. 3. THg concentrations in muscle vs liver (a) and MMHg concentration in the muscle vs IHg concentration in the liver (b) of 17 tilefish caught at different locations in the northern GoM.

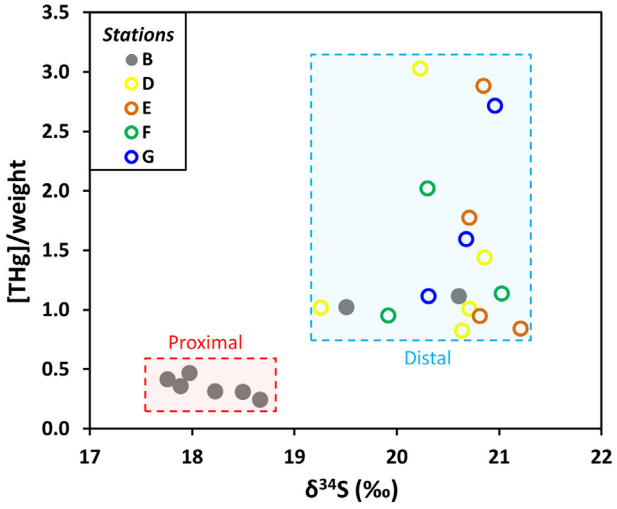

Fig. 4. [THg]/weight vs $\delta^{34}S$ in Tilefish muscles, showing 2 different pools between the distal area (>138 km from MR mouth) and the proximal area (<52 km form MR mouth). Two fish that were sampled near DWH and MR mouth (station B) belong to the distal pool.

stations clearly showed that a difference in trophic levels is not responsible for the different Hg bioaccumulation between these two areas. While no correlations were observed between $\delta^{34}S$ and MMHg at station B or other stations (Fig. S6), higher Hg concentrations were associated with higher $\delta^{34}S$ values (Fig. 4). This suggests that higher Hg bioaccumulation occurs in fish living in waters that show more marine sulphate signatures. Interestingly, we observed that two fish from station B had $\delta^{34}S$ signatures similar to fish from other stations. These two fish (DC-13-795 and DC-13-798) also showed higher THg/weight ratios and lower $\delta^{15}N$ signatures than other fish from station B (Table S5). It is possible that, while they were sampled close to the DWH and the MR mouth, these two fish spent the last years of their life in more distal waters. However, these fish were also smaller than all the other fishes sampled at stations B and potentially have different diet than larger/older ones. In the remaining manuscript, station B will be considered as "proximal" (i.e. close to the MR mouth) while stations D to G will be considered at "distal".

3.2.2. Hg isotopic composition

Delta values for all muscle ($n = 23$) and liver samples ($n = 9$) are provided in Table S5. Overall, $\delta^{202}Hg$ in tilefish muscle ranged from −0.60 to 0.52‰ and $\Delta^{199}Hg$ ranged from 0.60 to 1.15‰. Hg MDF and MIF signatures in tilefish muscle were significantly different between stations close (47 km) and far (≥109 km) from the DWH. Tilefish muscles from station B displayed significantly lower $\delta^{202}Hg$ ($t = -6.78$ and $p < 0.00001$) and $\Delta^{199}Hg$ ($t = -5.19$ and $p = 0.00004$) values (−0.21 ± 0.21‰ and 0.75 ± 0.10‰, respectively, $n = 8$) than tilefish muscle from stations far from the DWH (0.29 ± 0.14‰ and 0.98 ± 0.10‰, respectively, $n = 15$) and $\Delta^{199}Hg$ was positively correlated to $\delta^{202}Hg$ ($p < 0.00001$, Fig. 5a). $\Delta^{199}Hg/\Delta^{201}Hg$ ratios were close to 1.3 (average 1.24 ± 0.05) for all tilefish muscle samples (Fig. 5b), this is consistent with the accumulation of MMHg that has been subjected to photodemethylation in the water column before its incorporation in the food chain (Bergquist and Blum, 2007). A significant and positive correlation was observed between the logarithm of THg concentration and $\delta^{202}Hg$ in tilefish muscle samples (Fig. S7), suggesting MDF during bioaccumulation (due to in-vivo demethylation (Perrot et al., 2016)) of MMHg in the muscle and/or binary sources mixing (Foucher et al., 2009; Perrot et al., 2010).

Overall, δ^{202} Hg in tilefish liver ranged from −0.93 to 0.15‰ and $\Delta^{199}Hg$ ranged from 0.47 to 1.05‰ (Table S5). As for muscle, Hg MIF signatures in tilefish liver were significantly different between the proximal area and stations located more offshore, with tilefish liver from station B displaying significantly lower $\Delta^{199}Hg$ values (0.57‰) than tilefish liver from stations far from the DWH (0.94 ± 0.09‰, n = 8). However, only a slight difference of MDF signature was observed between tilefish livers from station B and other stations ($\delta^{202}Hg$ = −0.23‰ (n = 1) and −0.09 ± 0.09‰ (n = 8), respectively). While fish from stations D, E, F, and G displayed a consistent and positive offset of $\delta^{202}Hg$ in the muscle relative to the liver ($\delta^{202}Hg_{muscle} - \delta^{202}Hg_{liver} = 0.41 \pm 0.17$‰), fish from station B had on average a negative offset ($\delta^{202}Hg_{muscle} - \delta^{202}Hg_{liver} = -0.17$). The MIF offset between muscle and liver of tilefish was slightly positive, with fish from station B having a slightly higher offset ($\Delta^{199}Hg_{muscle} - \Delta^{199}Hg_{liver} = 0.12$‰) than fish from stations D, E, F, and G (0.08 ± 0.04‰, n = 8). Overall, the MDF offset between muscle and liver becomes more positive with the distance to the MR mouth and DWH (Fig. S8a) and increases with Hg accumulation normalized to the size of the fish (Fig. S8b). In fish with higher levels of Hg

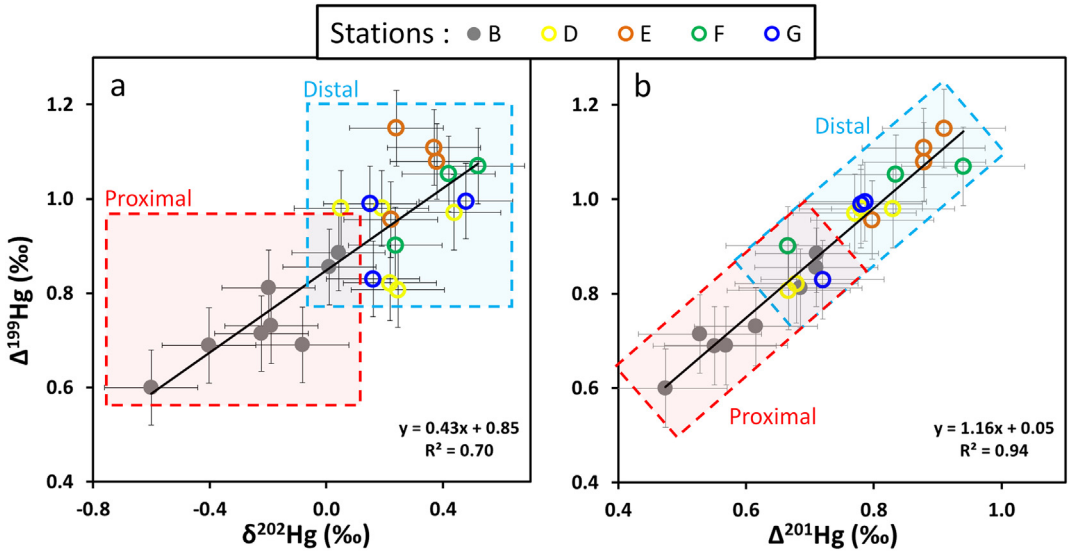

Fig. 5. $\Delta^{199}Hg$ vs $\delta^{202}Hg$ (a) and $\Delta^{199}Hg$ vs $\Delta^{201}Hg$ (b) in tilefish muscle, showing 2 different Hg isotopic pools between the distal area (>178 km from MR mouth) and the proximal area (<52 km form MR mouth). Error bars represent long-term uncertainties of analyses (2SD).

contamination (i.e. distal stations), this offset increased with increasing IHg concentration in the liver relative to MMHg concentration in the muscle (Fig. S8c) that is in agreement with MDF during MMHg demethylation to IHg and subsequent storage of IHg in the liver and the remaining MMHg in the muscle suggested for mammals (Perrot et al., 2016). Interestingly, liver of the fish from station B also showed a lower $\Delta^{199}Hg/\Delta^{201}Hg$ ratio (0.89), close to 1.0 ratio indicative of IHg photoreduction (Bergquist and Blum, 2007) than livers of fish from other stations (1.25 ± 0.05, close to 1.3 ratio indicative of MMHg photoreduction (Bergquist and Blum, 2007) (Fig. S9). Hence, we suggest that Hg in tilefish liver at distal stations mostly originated from MMHg demethylation (in-vivo) while tilefish from proximal stations can have a significant fraction of IHg in their liver directly taken up from prey and/or the water column and seabed.

3.3. Geographical variations of Hg bioaccumulation in tilefish from the northeastern GoM constrained with Hg and light stable isotopes

Lower Hg concentrations were observed in tissues of tilefish located close to the MR mouth and the DWH (proximal, MR-DWH, station B) than in tilefish located more offshore and northeast along the DeSoto Canyon (distal, Off-DSC, stations D, E, F, G). These geographical patterns were the same for light stable isotopes as well as for Hg isotopic composition in the fish tissues (Fig. 6). These are discussed with Hg concentrations to identify environmental factors potentially affecting Hg bioaccumulation in fish at different sites of the sampling area. Tilefish were sampled in 2012 and 2013, >2 years after the DWH. All tilefish were larger than 29 cm in standard length that indicates that they all were born before the DWH event, based on observed length/age ratios (Lombardi et al., 2010). According to the residence time of Hg species in the muscle and liver of fish (Trudel and Rasmussen, 1997), we assumed that the vast majority of MMHg and IHg measured in our samples was incorporated after the DWH event.

A previous study reported Hg, N and C isotopes in fish from the northern GoM and showed that coastal and oceanic fish species exhibited disconnected food webs and Hg sources (Senn et al., 2010), however no comparison between the same fish species in different areas was carried out. Still the authors showed that coastal fish had higher $\delta^{15}N$ and $\delta^{13}C$, and lower MMHg levels, $\delta^{202}Hg$ and $\Delta^{199}Hg$, than oceanic fish. They also observed a positive correlation between MMHg and $\delta^{13}C$ in coastal fish that was not observed for tilefish in our study. As for their study, we suggest that lower $\delta^{202}Hg$ and $\Delta^{199}Hg$ values in tilefish from MR-DWH area were due to lower photodemethylation efficiency than at distal stations due to limited light penetration close to the MR plume. All station depths (>200 m) were below the photic zone, and we argue here that different foraging depths for our sampling stations (range 204-333 m) did not play a role in the observed differences in Hg MIF signatures since higher $\Delta^{199}Hg$ values were observed in Off-DSC stations (range 255-337 m) than at station B (range 204-301 m), which contrasts with oceanic pelagic fish species (Blum et al., 2013; Madigan et al., 2018). Overall, depth differences between the sampling stations were not responsible for the differences observed in light and Hg stable isotopes nor in THg accumulation (Fig. S10).

It has been reported that the MR can be an important source of Hg for the GoM waters, in addition to direct Hg atmospheric deposition (Harris et al., 2012; Rice et al., 2009). Besides being relatively close to the DWH site (47 km), the station B was also located very close (52 km) to the mouth of MR compared to other stations (>178 km). Hence, at the MR-DWH station, even when water discharge is reduced, the MR plume still has a strong influence (Morey et al., 2003; Walker, 1996). However, if the MR is an important source of Hg for these stations, this does not explain why Hg concentrations in tilefish tissues were significantly lower than in tilefish tissues from other stations where less influence from the MR (mostly atmospheric deposition) should occur. Hence, direct Hg discharge from the MR is unlikely to explain the differences of Hg concentrations observed in tilefish of our study. Hg isotopic composition in sediments of the seafloor in our

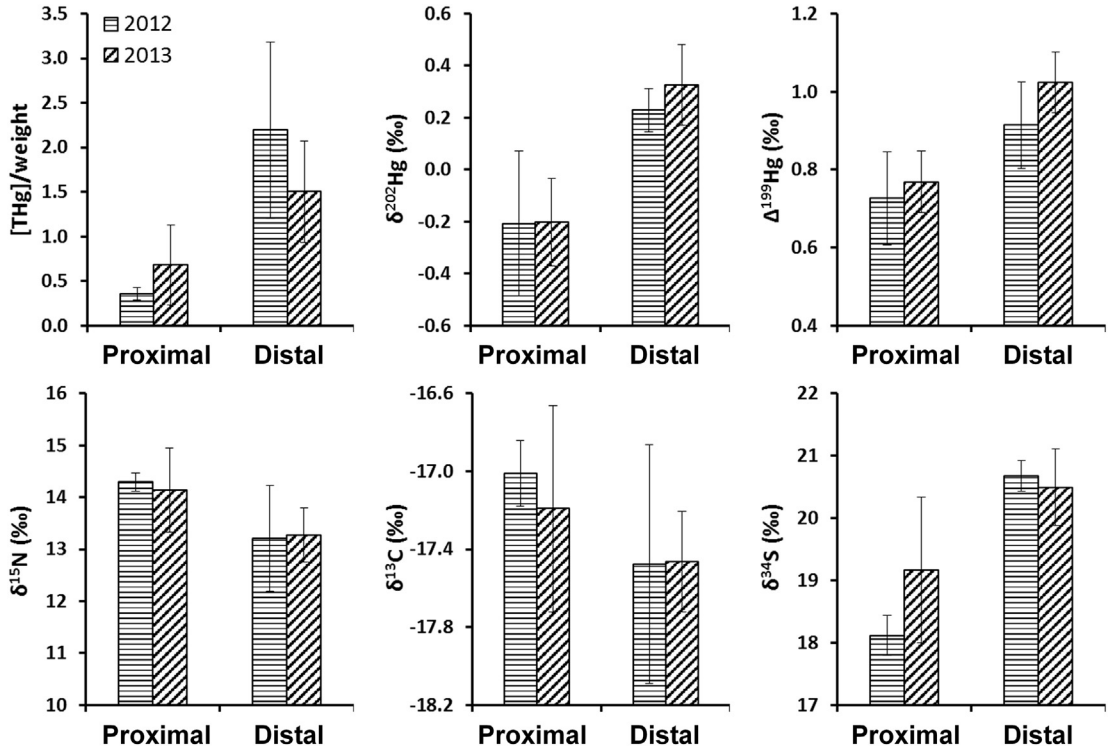

Fig. 6. 2012 and 2013 average values for total Hg concentrations (normalized to weight) (a), $\delta^{202}Hg$ (b), $\Delta^{199}Hg$ (c), $\delta^{15}N$ (d), $\delta^{13}C$ (e) and $\delta^{34}S$ (f), measured in muscles of Tilefish sampled at proximal stations (MR-DWH, station B) and fish sampled at distal stations (off-DSC, stations D, E, F, and G).

study area and the MR would also help to identify different Hg sources in tilefish. While no such data are available near our sampling sites, a few studies report Hg levels (Rice et al., 2009; Trefry et al., 2007) and stable isotopes (Brown et al., 2013) in sediments of the nGOM and in the MR sediments (Gray et al., 2015). Both coastal and upstream MR sediments showed slightly negative or near 0 values for Δ^{199}Hg, indicating Hg from geogenic and/or anthropogenic sources, while Hg in more distal and deep sea stations have slightly positive Δ^{199}Hg and higher δ^{202}Hg values than at coastal stations indicating a higher contribution of precipitation. Interestingly, this shift is also observed in Hg isotopic signatures in tilefish between the proximal area (station B) and other stations, but higher values are observed probably due to the fact that Hg can undergo multiple isotopic fractionation processes between the sediment and Hg storage in muscle [(Blum et al., 2014) and references herein]. Again, while the MR seems to be a significant source of Hg in sediments from the coastal area, this does not explain why lower Hg levels were encountered in tilefish from this area.

The MR is responsible for large inputs of freshwater and terrestrial material (inorganic and organic dissolved/particulate matter) and nutrients that lead to high biomass production and changes in redox conditions and salinity in the water column and sediments on the continental shelf near the MR mouth (Cardona et al., 2016; Dagg and Breed, 2003; Rabalais et al., 2002; Wang et al., 2004). Indeed, there is a significant decrease in nutrient, silicates, and hence turbidity, from the MR mouth to more distal waters (Fig. S11). The rapid decrease in nutrient concentration associated with an increase in salinity, especially within the first 100 km from the MR mouth (Cardona et al., 2016), can explain significantly higher δ^{15}N and lower δ^{34}S signatures observed at station MR-DWH than at Off-DSC stations. Decreasing δ^{15}N in low trophic levels as well as in fish populations has been recently reported along the shelf of the northeastern GoM, with increasing distance from the MR mouth (Radabaugh and Peebles, 2014).

Overall, we observed the C, N, and S isotopic signatures changing as a function of the distance from the MR mouth. Hence, both S and N (and C to a lesser degree) stable isotopic signatures in tilefish (Figs. 6 and S12) support the idea that the MR has a strong impact on the biogeochemistry of water and sediments in the shelf eastward off Louisiana. Hence, while recent studies showed the importance of Mississippi inputs on the West Florida Shelf (e.g. (Walsh et al., 2015) and reference herein), our results are still more consistent with a limited influence at the NE mouth of the DSC (i.e. stations >109 km from DWH). This is supported by the type of sediment (where tilefish live and feed on) present at station B (terrigenous clay), while other stations are characterized with calcareous sediments (offshore signature) (Balsam and Beeson, 2003), as well as differences in nutrient loads (Cardona et al., 2016) (also see Fig. S11). This change in sediment nature potentially affects Hg biogeochemistry and, hence, Hg bioavailability at the base of the food chain.

A recent study on red snapper (*Lutjanus campechanus*) from the northern GoM reports that higher Hg levels in fish with limited riverine influence are also associated with higher δ^{34}S and suggests that terrestrial inputs associated with hypoxia near the mouth of the MR inhibits MMHg production and further bioaccumulation in food chains (Zapp Sluis et al., 2013). Indeed, high levels of sulphide and terrestrial particulate organic matter should reduce MMHg production and bioavailability, rather than enhance Hg(II) reduction (Zhang et al., 2011; Zhu et al., 2018). Conversely, it seems that Hg bioavailability and subsequent bioaccumulation into food webs is enhanced in oligotrophic waters with marine dissolved organic matter associated with freshly deposited Hg (Chiasson-Gould et al., 2014; Schartup et al., 2015). This phenomenon could be of particular importance in our study area where elevated precipitation (the main GoM Hg source (Rice et al., 2009)) occurs (Fig. S11). Higher inputs of freshwater and particulate material from MR (lower salinity, higher turbidity and nutrient load, see Fig. S11) is corroborated by lower δ^{34}S, Δ^{199}Hg and δ^{202}Hg, and higher δ^{15}N values (see above) observed at station B (Fig. 6 and Fig. S12). In addition, the blooms of biomass near the MR mouth should reduce MMHg concentrations at the base of the food chains (biodilution) and further bioaccumulation (Harmelin-Vivien et al., 2009; Wu et al., 2019), although the opposite has been observed in some fresh water systems (Todorova et al., 2015). Hence, we suggest that lower Hg concentrations (and [Hg] normalized to weight or length) in fish living at proximal stations are due to limited Hg bioavailability at the base of the food chain as a result of terrestrial inputs of particles and nutrients from the Mississippi River.

The DWH event in 2010 released large amounts of oil that has largely affected the biogeochemistry of both the waters and the seafloor of the Gulf of Mexico (Hastings et al., 2016; Joye, 2015), impacting local ecosystems (Ainsworth et al., 2018; Crowe et al., 2014). Oil carbon has been shown to enter the base of food chains (Cherrier et al., 2014; Graham et al., 2010) and has modified composition and interaction of microbial communities (Lu et al., 2012; Ziervogel et al., 2016) that are both key parameters controlling MMHg production/degradation and bioaccumulation through higher trophic levels.

As demersal fish, tilefish forage on prey on and in GoM sediments, and a recent study indicates that this type of fish has been significantly impacted by the DWH, leading to a biomass decrease up to 70% and enhanced starvation (Ainsworth et al., 2018). Hence, reduced feeding rate and low health status can have significantly reduced Hg accumulation in MR-DWH tilefish. Other studies report changes in diet in some fish following the DWH event (Quintana-Rizzo et al., 2015; Tarnecki and Patterson III, 2015), one of them reporting a significant increase in δ^{13}C and δ^{15}N, and a decrease in δ^{34}S, in red snapper after the oil spill (Tarnecki and Patterson III, 2015) that are close to the offset of light stable isotopes average values between tilefish at MR-DWH station and Off-DSC stations. However, and unfortunately, we do not have light or Hg stable isotopes data prior to the DWH for tilefish in order to definitely confirm pre- to post-spill changes specific to tilefish.

Stimulation of bacterial activity following the DWH event due to both oil release and the addition of chemical dispersants (Kleindienst et al., 2015), especially sulphate reduction (Kimes et al., 2014), could also explain the lower δ^{34}S values observed at MR-DWH station. For example, enhanced reducing conditions on the seafloor after the DWH have been reported (Brooks et al., 2015; Hastings et al., 2016). Since a large variety of SRBs are able to reduce, methylate and demethylate Hg (Bridou et al., 2011; Hu et al., 2013; King et al., 2000), but only ones possessing specific genes can significantly produce MMHg (Parks et al., 2013), lower MMHg levels observed in tilefish at MR-DWH stations would suggest higher net MMHg demethylation and IHg reduction than MMHg production in this area. However, and as previously stated, more reducing conditions should already occur at MR-DWH station than at Off-DSC stations due to the proximity of the MR mouth.

Sedimentation rates and associated oil accumulation on the seafloor after the DWH blowout (i.e. marine snow) (Passow et al., 2012) have been significantly enhanced locally in the DeSoto Canyon by the terrestrial discharge from the MR (Babcock-Adams et al., 2017; Brooks et al., 2015; Daly et al., 2016; Hastings et al., 2016; Romero et al., 2017; Romero et al., 2015). Indeed, the combination of MR nutrients and particles inputs with oil is suggested to have increased microbial blooms, anoxia, and sedimentation rates at river-proximal than river-distal areas (Daly et al., 2016) (Edwards et al., 2011) that would result in increased Hg biodilution, Hg reduction and demethylation and limited Hg bioavailability, respectively (see discussion above). Marine snow from MR-oil interaction is also likely to have impacted fish feeding strategies and/or health due to change in food webs structures. Hence, we suggest that the MR discharge and the DWH event could have interacted together to provide even more limited Hg bioaccumulation in tilefish at stations located on the Louisiana Shelf.

4. Conclusions

Our study provided a multi-isotopic analyses to decipher Hg bioaccumulation in demersal fish from the northeastern Gulf of Mexico

following the DWH oil spill. Our data show that Hg bioaccumulation was significantly reduced in fish located on the Louisiana shelf break. Terrestrial discharge from the Mississippi River was identified as the main driver of limited Hg bioavailability to local food webs, and increased sedimentation rates as well as lower fish health status due to the oil release are likely to have amplified this phenomenon. Mercury bioaccumulation in fish from more oligotrophic waters (off the Alabama and Florida shelves), even if these areas may have also been affected by the DWH event (Romero et al., 2017; Weisberg et al., 2016), was high and most of the fish had critical Hg levels that exceed safety thresholds for daily consumption. This highlights the fact that species-level targeting to establish Hg guidelines is not sufficient in the GoM and supports the need for further local and regional investigations.

Mercury isotopic signatures indicate that, in tilefish with relatively low Hg concentrations in both muscle and liver, an important contribution of Hg is from inorganic Hg accumulation from various sources (food and water column, MR discharge). On the other hand, tilefish with higher Hg bioaccumulation rates (mostly MMHg), Hg MIF signatures indicate that both IHg and MMHg in the liver mostly arise from MMHg demethylation from which they are respectively product and residual components. Relationships were significant between Hg species and Hg isotopic composition between the muscle and the liver, supporting the idea that fish can significantly demethylate MMHg at a certain level of exposure and retain a fraction of the product, IHg, in the liver.

The influence of the Mississippi River discharge, the absence of Pre-spill Hg data and rare geochemical studies for tilefish in this area make estimating the oil spill role on Hg bioaccumulation difficult, however our study showed that we could not reject the null hypothesis that the DWH had a significant role in reducing Hg accumulation in fish due to marine snow and its associated hydrocarbon toxicity effects.

Acknowledgements

The authors acknowledge the Deep-C consortium and the Gulf of Mexico Research Initiative (GoMRI) for funding, Bruce Barnett for C and N isotope analysis, Jeffrey Chanton for S isotope analysis, and RV Apalachee and RV Weatherbird II teams for fishery independent survey efforts. Fish samples were collected under the approval of Florida State University Animal Care and Use Committee protocol #1111. The National High Magnetic Field Laboratory is supported by National Science Foundation through NSF/DMR-1157490 and the State of Florida.

Appendix A. Supplementary data

Supplementary data to this article can be found online at https://doi.org/10.1016/j.scitotenv.2019.02.295.

References

Adams, D.H., McMichael, R.H., Henderson, G.E., 2003. Mercury levels in marine and estuarine fishes of Florida 1989-2001, Florida marine research institute technical report TR-9, 2nd ed. rev.

Aiken, K.A., Collette, B., Dooley, J., Kishore, J., Marechal, R., Pina Amargos, F., Singh-Renton, S., 2015. *Lopholatilus chamaeleonticeps*. The IUCN red list of threatened species, 2015: e.T16545046A16546277.

Ainsworth, C.H., Paris, C.B., Perlin, N., Dornberger, L.N., Patterson III, W.F., Chancellor, E., Murawski, S., Hollander, D., Daly, K., Romero, I.C., Coleman, F., Perryman, H., 2018. Impacts of the Deepwater Horizon oil spill evaluated using an end-to-end ecosystem model. PLoS One 13 (1), e0190840.

Babcock-Adams, L., Chanton, J.P., Joye, S., Medeiros, P.M., 2017. Hydrocarbon composition and concentrations in the Gulf of Mexico sediments in the 3 years following the Macondo well blowout. Environ. Pollut. 229, 329–338.

Balsam, W.L., Beeson, J.P., 2003. Sea-floor sediment distribution in the Gulf of Mexico. Deep-Sea Res. I 50, 1421–1444.

Barkay, T., Gillman, M., Turner, R.T., 1997. Effects of dissolved organic carbon and salinity on bioavailability of mercury. Appl. Environ. Microbiol. 63 (1), 4267–4271.

Bergquist, B.A., Blum, J.D., 2007. Mass-dependant and –independent fractionation of Hg isotopes by photoreduction in aquatic systems. Science 318, 417–420.

Black, F.J., Poulin, B.A., Flegal, A.R., 2012. Factors controlling the abiotic demethylation of monomethylmercury in surface waters. Geochim. Cosmochim. Acta 84, 492–507.

Blum, J.D., Bergquist, B.A., 2007. Reporting of variations in the natural isotopic composition of mercury. Anal. Bioanal. Chem. 388, 353–359.

Blum, J.D., Popp, B.N., Drazen, J.C., Choy, C.A., Johnson, M.W., 2013. Methylmercury production below the mixed layer in the North Pacific Ocean. Nat. Geosci. 6, 879–884.

Blum, J.D., Sherman, L.S., Johnson, M.W., 2014. Mercury isotopes in earth and environmental sciences. Annu. Rev. Earth Planet. Sci. 42, 249–269.

Brenna, J.T., Corso, T.N., Tobias, H.J., Caimi, R.J., 1997. High-precision continuous-flow isotope ratio mass spectrometry. Mass Spectrom. Rev. 16, 227–258.

Brette, F., Machado, B., Cros, C., Incardona, J.P., Scholz, N.L., Block, B.A., 2014. Crude oil impairs cardiac excitation-contraction coupling in fish. Science 343 (6172), 772–776.

Bridou, R., Monperrus, M., Rodriguez-Gonzalez, P., Guyoneaud, R., Amouroux, D., 2011. Simultaneous determination of mercury methylation and demethylation capacities of various sulfate-reducing bacteria using species-specific isotopic tracers. Environ. Toxicol. Chem. 30, 1–8.

Brooks, G.R., Larson, R.A., Schwing, P.T., Romero, I., Moore, C., Reichart, G.-J., Jilbert, T., Chanton, J.P., Hastings, D.W., Overholt, W.A., Marks, K.P., Kotska, J.E., Holmes, C.W., Hollander, D., 2015. Sedimentation pulse in the NE Gulf of Mexico following the 2010 DWH Blowout. PLoS One 10 (7), e0132341.

Brown Jr., G.E., Sleeper, K., Johnson, M.W., Blum, J.D., Cizdziel, J.V., 2013. Mercury concentrations, speciation, and isotopic composition in sediment from a cold seep in the northern Gulf of Mexico. Mar. Pollut. Bull. 77, 308–314.

Cabana, G., Rasmussen, J.B., 1996. Comparison of aquatic food chains using nitrogen isotopes. Proc. Natl. Acad. Sci. U. S. A. 93 (20), 10844–10847.

Cai, Y., Rooker, J.R., Gill, G.A., Turner, J.P., 2007. Bioaccumulation of mercury in pelagic fishes from the northern Gulf of Mexico. Can. J. Fish. Aquat. Sci. 64, 458–469.

Cardona, Y., Bracco, A., Villareal, T.A., Subramaniam, A., Weber, S.C., Montoya, J.P., 2016. Highly variable nutrient concentrations in the Northern Gulf of Mexico. Deep-Sea Research Part II: Topical Studies in Oceanography 129, 20–30.

Carr, M., Jardine, T.D., Doig, L.E., Jones, P.D., Bharadwaj, L., Tendler, B., Cheletat, J., Cott, P., Lindenschmidt, K.-E., 2017. Stable sulfur isotopes identify habitat-specific foraging and mercury exposure in a highly mobile fish community. Sci. Total Environ. 586, 338–346.

Chanton, J., Zhao, J., Rosenheim, B.E., Joye, S., Bosman, S., Brunner, C., Yeager, K.M., Dierks, A.R., Hollander, D., 2015. Using natural abundance radiocarbon to trace the flux of petrocarbon to the seafloor following the Deepwater Horizon oilspill. Environmental Science & Technology Letters 49 (2), 847–854.

Cherrier, J., Sarkodee-Adoo, J., Guilderson, T.P., Chanton, J.P., 2014. Fossil carbon in particulate organic matter in the Gulf of Mexico following the Deepwater Horizon event. Environmental Science & Technology Letters 1 (1), 108–112.

Chiasson-Gould, S.A., Blais, J.M., Poulain, A.J., 2014. Dissolved organic matter kinetically controls mercury bioavailability to bacteria. Environmental Science & Technology 48 (6), 3153–3161.

Churchill, D.A., Heithaus, M.R., Vaudo, J.J., Grubbs, R.D., Gastrich, K., Castro, J.I., 2015. Trophic interactions of common elasmobranchs in deep-sea communities of the Gulf of Mexico revealed through stable isotope and stomach content analysis. Deep-Sea Research Part II: Topical Studies in Oceanography 115, 92–102.

Coelho, G., Clark, J., Aurand, D., 2013. Toxicity testing of dispersed oil requires adherence to standardized protocols to assess potential real world effects. Environ. Pollut. 177, 185–188.

Compeau, G.C., Bartha, R., 1985. Sulfate-reducing bacteria: principal methylators of mercury in anoxic estuarine sediments. Appl. Environ. Microbiol. 50 (2), 498–502.

Crowe, K.M., Newton, J.C., Kaltenboeck, B., Johnson, C., 2014. Oxidative stress responses of. Gulf Killifish exposed to hydrocarbons from the Deepwater Horizon oil spill: Potential implications for aquatic food resources Environmental Toxicology and Chemistry 33 (2), 370–374.

Dagg, M.J., Breed, G.A., 2003. Biological effects of Mississippi River nitrogen on the northern Gulf of Mexico - a review and synthesis. J. Mar. Syst. 43, 133–152.

Dagg, M.J., Bianchi, T., McKee, B., Powell, R., 2008. Fates of dissolved and particulate materials from the Mississippi river immediately after discharge into the northern Gulf of Mexico, USA, during a period of low wind stress. Cont. Shelf Res. 28, 1443–1450.

Daly, K.L., Passow, U., Chanton, J., Hollander, D., 2016. Assessing the impacts of oil-associated marine snow formation and sedimentation during and after the Deepwater Horizon oil spill. Anthropocene 13, 18–33.

Das, R., Salters, V.J.M., Odom, A.L., 2009. A case for in vivo mass-independant fractionation of mercury isotopes in fish. Geochemistry Geophysics Geosystems 10 (11), 1–12.

Dubansky, B., Whitehead, A., Miller, J.T., Rice, C.D., Galvez, F., 2013. Multitissue molecular, genomic, and developmental effects of the Deepwater Horizon oil spill on resident gulf Killifish (*Fundulus grandis*). Environmental Science & Technology 47, 5074–5082.

Dubinsky, E.A., Conrad, M.E., Chakraborty, R., Bill, M., Borglin, S.E., Hollibaugh, J.T., Mason, O.U., Piceno, Y.M., Reid, F.C., Stringfellow, W.T., Tom, L.M., Hazen, T.C., Andersen, G.L., 2013. Succession of hydrocarbon-degradating bacteria in the aftermath of the *Deepwater Horizon* oil spill in the Gulf of Mexico. Environmental Science & Technology 47 (19), 10860–10867.

Edwards, B.R., Reddy, C.M., Camilli, R., Carmichael, C.A., Longnecker, K., Van Mooy, B.A.S., 2011. Rapid microbial respiration of oil from the *Deepwater Horizon* spill in offshore surface waters of the Gulf of Mexico. Environ. Res. Lett. 6, 035301 (9pp).

Fitzgerald, T.P., Gohlke, J.M., 2014. Contaminant levels in Gulf of Mexico reef fish after the *Deepwater Horizon* oil spill as measured by a fishermen-led testing program. Environmental Science & Technology 48 (3), 1993–2000.

Fitzgerald, W.F., Lamborg, C.H., Hammerschmidt, C.R., 2007. Marine biogeochemical cycling of mercury. Chem. Rev. 107 (2), 641–662.

Foucher, D., Ogrinc, N., Hintelmann, H., 2009. Tracing mercury contamination from the Idrija mining region (Slovenia) to the Gulf of Trieste using Hg isotope ratios measurements. Environmental Science & Technology 43 (1), 33–39.

Graham, W.M.C., Carmichael, R.H., D'Ambra, I., Patterson, H.K., Linn, L.J., Hernandez Jr., F.J., 2010. Oil carbon entered the coastal planktonic food web during the Deepwater Horizon oil spill. Environ. Res. Lett. 5, 1–6.

Gray, J.E., Van Metre, P.C., Pribil, M.J., Horowitz, A.J., 2015. Tracing historical trends of Hg in the Mississippi River using Hg concentrations and Hg isotopic compositions in a lake sediment core, Lake Whittington, Mississippi, USA. Chem. Geol. 395, 80–87.

Harmelin-Vivien, M., Cossa, D., Crochet, S., Banaru, D., Letourneur, Y., Mellon-Duval, C., 2009. Difference of mercury bioaccumulation in red mullets from the northwestern. Mediterranean and Black seas Marine Pollution Bulletin 58 (5), 679–685.

Harris, R., Pollman, C.D., Landing, W.M., Evans, D.W., Axelrad, D., Hutchinson, D., Morey, S.L., Rumbold, D., Dukhovskoy, D., Adams, D.H., Vijayaraghavan, K., Holmes, C., Atkinson, R.D., Myers, T., Sunderland, E., 2012. Mercury in the Gulf of Mexico: sources to receptors. Environ. Res. 119, 42–52.

Hastings, D.W., Schwing, P.T., Brooks, G.R., Larson, R.A., Monford, J.L., Roeder, T., Quinn, K.A., Bartlett, T., Romero, I.C., Hollander, D.J., 2016. Changes in sediment redox conditions following the BP DWH blowout event. Deep-Sea Research Part II: Topical Studies in Oceanography 129, 167–178.

Havelkova, M., Dusek, L., Némethova, D., Poleszczuk, G., Svobodova, Z., 2008. Comparison of mercury distribution between liver and muscle - a biomonitoring of fish from lightly and heavily contaminated localities. Sensors 8, 4095–4109.

Hu, H., Lin, H., Zheng, W., Rao, B., Feng, X., Liang, L., Elias, D.A., Gu, B., 2013. Mercury reduction and cell-surface adsorption by *Geobacter sulfurreducens* PCA. Environmental Science & Technology 47 (19), 10922–10930.

Incardona, J.P., Gardner, L.D., Linbo, T.L., Brown, T.L., Esbaugh, A.J., Mager, E.M., Stieglitz, J.D., French, B.L., Labenia, J.S., Laetz, C.A., Tagal, M., Sloan, C.A., Elizur, A., Benetti, D.D., Grosell, M., Block, B.A., Scholz, N.L., 2014. Deepwater. *Horizon* crude oil impacts the developing hearts of large predatory pelagic fish Proceedings of the National Academy of Sciences of the United States of America 111 (15), 1510–1518.

Jones, R.S., Gutherz, E.J., Nelson, W.R., Matlock, G.C., 1989. Burrow utilization by yellowedge grouper, *Epinephelus flavolimbatus*, in the northwestern Gulf of Mexico. Environ. Biol. Fish 26, 277–284.

Joye, S.B., 2015. Deepwater Horizon, 5 years on. Science 349 (6248), 592–593.

Joye, S.B., Teske, A.P., Kostka, J.E., 2014. Microbial dynamics following the Macondo oil well blowout across Gulf of Mexico environments. BioScience 64 (9), 766–777.

Jung, J.-H., Yim, U.-H., Han, G.-M., Shim, W.J., 2009. Biochemical changes in rockfish, *Sebastes schlegeli*, exposed to dispersed crude oil. Comparative biochemistry and Physiology, Part C 150, 218–223.

Karimi, R., Fitzgerald, T.P., Fisher, N.S., 2012. A Quantitative Synthesis of Mercury in Commercial Seafood and Implications for Exposure in the United States Environmental Health Perspectives 120 (11), 1512–1519.

Khan, M.A.K., Wang, F., 2010. Chemical demethylation of methylmercury by selenoamino acids. Chemical Research and Toxicology 23 (7), 1202–1206.

Kimes, N., Callaghan, A.V., Sulfita, J.M., Morris, P.J., 2014. Microbial transformations of the Deepwater Horizon oil spill - past, present, and future perspectives. Front. Microbiol. 5 (603). https://doi.org/10.3389/fmicb.2014.00603.

King, J.K., Kostka, J.E., Frischer, M.E., Saunders, F.M., 2000. Sulfate-reducing bacteria methylate mercury at variable rates in pure culture and in marine sediments. Appl. Environ. Microbiol. 66 (6), 2430–2437.

Kleikemper, J., Schroth, M.H., Bernasconi, S.M., Brunner, B., Zeyer, J., 2003. Sulfur isotope fractionation during growth of sulfate-reducing bacteria on various carbon sources. Geochim. Cosmochim. Acta 68 (23), 4891–4904.

Kleindienst, S., Paul, J.H., Joye, S., 2015. Using dispersants after oil spills: impacts on the composition and activity of microbial communities. Nat. Rev. Microbiol. 13, 388–396.

Kritee, K., Blum, J.D., Reinfelder, J.R., Barkay, T., 2013. Microbial stable isotope fractionation of mercury: a synthesis of present understanding and future directions. Chem. Geol. 336, 13–25.

Kwon, S.Y., Blum, J.D., Carvan, M.J., Basu, N., Head, J.A., Madenijan, C.P., David, S.R., 2012. Absence of fractionation of mercury isotopes during trophic transfer of methylmercury to freshwater fish in captivity. Environmental Science & Technology 46 (14), 7527–7534.

Kwon, S.Y., Blum, J.D., Chirby, M.A., Chesney, E.J., 2013. Application of mercury isotopes for tracing trophic transfer and internal distribution of mercury in marine fish feeding experiments. Environ. Toxicol. Chem. 32 (10), 2322–2330.

Liu, Y., Weisberg, R.H., Hu, C., Kovach, C.W., Riethmuller, 2011. Evolution of the Loop Current System During the Deepwater Horizon Oil Spill Event as Observed With Drifter and Satellites: A record-Breaking enterprise. Goephysical Monograph Series, 195 https://doi.org/10.1029/2011GM001127.

Lombardi, L.A., Fitzhugh, G., Lyon, H., 2010. Golden tilefish (*Lopholatilus chamaeleonticeps*) age, growth, and reproduction from the northeastern Gulf of Mexico: 1985, 1997–2009, Southeast Data, Assessment and Review, North Charleston, SC, USA.

Lu, Z., Deng, Y., Van Nostrand, J.D., He, Z., Voordeckers, J., Zhou, A., Lee, Y.-J., Mason, O.U., Dubinsky, E.A., Chavarria, K.L., Tom, L.M., Fortney, J.L., Lamendella, R., Jansson, J.K., D'haeseleer, P., Hazen, T.C., Zhou, J., 2012. Microbial gene functions enriched in the Deepwater Horizon deep-sea oil plume. International Society for Microbial Ecology, 6: 451-460.

MacDonald, I.R., Garcia-Pineda, O., Beet, A., Daneshgar Asl, S., Feng, L., Graettinger, G., French-McCay, D., Holmes, J., Hu, C., Huffer, F., Leifer, I., Muller-Karger, F., Solow, A., Silva, M., Swayze, G., 2015. Natural and unnatural oil slicks in the Gulf of Mexico. Journal of Geophysical Research: Oceans 120, 8364–8380.

Madigan, D.J., Li, M., Yin, R., Baumann, H., Snodgrass, O.E., Dewar, H., Krabbenhoft, D.P., Baumann, Z., Fisher, N.S., Balcom, P., Sunderland, E.M., 2018. Mercury stable isotopes reveal influence of foraging depth on mercury concentrations and growth in Pacific Bluefin tuna. Environmental Science & Technology 52 (11), 6256–6264.

Mager, E.M., Esbaugh, A.J., Stieglitz, J.D., Hoenig, R., Bodinier, C., Incardona, J.P., Scholz, N.L., Benetti, D.D., Grosell, M., 2014. Acute embryonic or juvenile exposure to *Deepwater Horizon* crude oil impairs the swimming performance of Mahi-Mahi (*Coryphaena hippurus*). Environmental Science & Technology 48 (12), 7053–7061.

Mendelssohn, I.A., Andersen, G.L., Baltz, D.M., Caffey, R.H., Carman, K.R., Fleeger, J.W., Joye, S.B., Lin, Q., Maltby, E., Overton, E.B., Rozas, L.P., 2012. Oil impacts on coastal wetlands: implications for the Mississippi River Delta ecosystem after the *Deepwater Horizon* oil spill. BioScience 62 (6), 562–574.

Morey, S.L., Schroeder, W.W., O'Brien, J.J., Zavala-Hidalgo, J., 2003. The annual cycle of riverine influence in the eastern Gulf of Mexico basin. Geophys. Res. Lett. 30 (16), 1867.

NMFS, 2017. Fisheries of the United States, 2016, National Marine Fisheries Service. U.S. Department of Commerce, NOAA Current Fishery Statistics No. 2016. Available at:. https://www.st.nmfs.noaa.gov/commercial-fisheries/fus/fus16/index.

NOAA, 1999. Essential Fish Habitat Source Document: Tilefish, *Lopholatilus chamaeleonticeps*, Life History and Habitat Characteristics. U.S. Department of Commerce, National Oceanic and Atmospheric Administration, National Marine Fisheries Service, Woods Hole, Massachusetts.

NOAA, 2011. Fisheries of the United States 2010. U.S. Department of Commerce, National Oceanic and Atmospheric Administration, National Marine Fisheries Service, Silver Spring, Maryland.

Pandey, S.K., Kim, K.-H., Yim, U.-H., Jung, M.-C., Kang, C.-H., 2009. Airborne mercury pollution from a large oil spill accident on the west coast of Korea. J. Hazard. Mater. 164, 380–384.

Parks, J.M., Johs, A., Podar, M., Bridou, R., Hurt, R.A., Smith, S.D., Tomanicek, S.J., Qian, Y., Brown, S.D., Brandt, C.C., Palumbo, A.V., Smith, J.C., Wall, J.D., Elias, D.A., Liang, L., 2013. The genetic basis for bacterial mercury methylation. Science 339, 1332–1335.

Passow, U., Ziervogel, K., Asper, V., Diercks, A., 2012. Marine snow formation in the aftermath of the Deepwater Horizon oilspill in the Gulf of Mexico. Environ. Res. Lett. 7, 1–11.

Paul, J.H., Hollander, D., Coble, P., Daly, K.L., Murasko, S., English, D., Basso, J., Delaney, J., McDaniel, L., Kovach, C.W., 2013. Toxicity and mutagenicity of Gulf of Mexico waters during and after the Deepwater Horizon oil spill. Environmental Science & Technology 47 (17), 9651–9659.

Pellerin, A., Anderson-Trocmé, L., Whyte, L.G., Zane, G.M., Wall, J.D., Wing, B.A., 2015. Sulfur isotope fractionation during the evolutionary adaptation of a sulfate-reducing bacterium. Appl. Environ. Microbiol. 81 (8), 2676–2689.

Perrot, V., Epov, V.N., Pastukhov, M.V., Grebenshchikova, V.I., Zouiten, C., Sonke, J.E., Husted, S., Donard, O.F.X., Amouroux, D., 2010. Tracing Sources and Bioaccumulation of Mercury in Fish of Lake Baikal-Angara River Using Hg Isotopic Composition Environmental Science & Technology 44 (21), 8030–8037.

Perrot, V., Pastukhov, M.V., Epov, V.N., Husted, S., Donard, O.F.X., Amouroux, D., 2012. Higher mass-independent fractionation of methylmercury in the pelagic food web of Lake Baikal (Russia). Environmental Science & Technology 46 (11), 5902–5911.

Perrot, V., Masbou, J., Pastukhov, M.V., Epov, V.N., Berail, S., Becker, P.R., Sonke, J.E., Amouroux, D., 2016. Natural Hg isotopic composition of different Hg compounds in mammal tissues as a proxy for in vivo breakdown of toxic methylmercury. Metallomics https://doi.org/10.1039/c5mt00286a.

Poje, A.C., Ozgokmen, T.M., Lipphardt Jr., B.L., Haus, B.K., Ryan, E.H., Haza, A.C., Jacobs, G.A., Reniers, A.J.H.M., Josefina Olascoaga, M., Novelli, G., Griffa, A., Beron-Vera, F.J., Chen, S.S., Coelho, E., Hogan, P.J., Kirwan Jr., A.D., Huntley, H.S., Mariano, A.J., 2014. Submesoscale dispersion in the vicinity of the *Deepwater Horizon* spill. Proc. Natl. Acad. Sci. U. S. A. 111 (35), 12693–12698.

Post, D.M., 2002. Using stable isotopes to estimate trophic position: models, methods, and assumptions. Ecology 83 (3), 703–718.

Prince, R.C., Parkerton, T.F., 2014. Comment on "toxicity and mutagenicity of Gulf of Mexico waters during and after the Deepwater Horizon oilspill". Environmental Science & Technology 48 (6), 3591–3592.

Quintana-Rizzo, E., Torres, J.J., Ross, S.W., Romero, I., Watson, K., Goddard, E.H.D., 2015. $\delta^{13}C$ and $\delta^{15}N$ in deep-living fishes and shrimps after the Deepwater Horizon oil spill, Gulf of Mexico. Mar. Pollut. Bull. 94, 241–250.

Rabalais, N.N., Turner, R.E., Dortch, Q., Justic, D., Bierman Jr., V.J., Wiseman Jr., W.J., 2002. Nutrient-enhanced productivity in the northern Gulf of Mexico. Hydrobiologia 475-476, 39–63.

Radabaugh, K.R., Peebles, E.B., 2014. Multiple regression models of $\delta^{13}C$ and $\delta^{15}N$ for fish populations in the eastern Gulf of Mexico. Cont. Shelf Res. 84, 158–168.

Ravichandran, M., 2004. Interactions between mercury and dissolved organic matter - a review. Chemosphere 55, 319–331.

Rebich, R.A., Houston, N.A., Mize, S.V., Pearson, D.K., Ging, P.B., Hornig, C.E., 2011. Sources and delivery of nutrients to the northwestern. Gulf of Mexico from streams in the south-central United States Journal of the American Water Resources Association 47 (5), 1061–1086.

Reddy, C.M., Arey, J.S., Seewald, J.S., Sylva, S.P., Lemkau, K.L., Nelson, R.K., Carmichael, C.A., McIntyre, C.P., Fenwick, J., Ventura, G.T., Van Mooy, B.A.S., Camilli, R., 2012. Composition and fate of gas and oil released to the water column during the *Deepwater Horizon* oil spill. Proc. Natl. Acad. Sci. U. S. A. 109 (50), 20229–20234.

Rees, C.E., Jenkins, W.J., Monster, J., 1978. The sulphur isotopic composition of ocean water sulphate. Geochim. Cosmochim. Acta 42 (4), 377–381.

Rice, G.E., Senn, D.B., Shine, J.P., 2009. Relative importance of atmospheric and riverine mercury sources to the Northern Gulf of Mexico. Environmental Science & Technology 43 (2), 415–422.

Rodriguez-Gonzalez, P., Epov, V.N., Bridou, R., Tessier, E., Guyoneaud, R., Monperrus, M., Amouroux, D., 2009. Species-specific stable isotope fractionation of mercury during Hg(II) methylation by an anaerobic bacteria (Desulfobulbus propionicus) under dark conditions. Environmental Science & Technology 43 (24), 9183–9188.

Romero, I.C., Schwing, P.T., Brooks, G.R., Larson, R.A., Hastings, D.W., Ellis, G., Goddard, E., Hollander, D., 2015. Hydrocarbons in Depe-Sea Sediments following the 2010 Deepwater Horizon Blowout in the Northeast Gulf of Mexico. PLoS One 10 (5), e01238371.

Romero, I., Toro-Farmer, G., Dierks, A.R., Schwing, P., Muller-Karger, F., Murawski, S.A., Hollander, D.J., 2017. Large-scale deposition of weathered oil in the Gulf of Mexico following a deep-water oil spill. Environ. Pollut. 228, 179–189.

Schartup, A.T., Ndu, U., Balcom, P.H., Mason, R.P., Sunderland, E., 2015. Contrasting effects of marine and terrestrially derived dissolved organic matter on mercury speciation and bioavailability in seawater. Environmental Science & Technology 49 (10), 5965–5972.

Senn, D.B., Chesney, E.J., Blum, J.D., Bank, M.S., Maage, A., Shine, J.P., 2010. Stable isotope (N, C, Hg) study of methylmercury sources and trophic transfer in the northern Gulf of Mexico. Environmental Science & Technology 44 (5), 1630–1637.

Sherman, L.S., Blum, J.D., Franzblau, A., Basu, N., 2013. New insight into biomarkers of human mercury exposure using naturally occurring mercury stable isotopes. Environmental Science & Technology 47 (7), 3403–3409.

Sim, M.S., Ono, S., Donovan, K., Templer, S.P., Bosak, T., 2011. Effect of electron donors on the fractionation of sulfur isotopes by a marine Desulfovibrio sp. Geochim. Cosmochim. Acta 75, 4244–4259.

Spier, C., Stringfellow, W.T., Hazen, T.C., Conrad, M.E., 2013. Distribution of hydrocarbons released during the 2010 MC252 oil spill in deep offshore waters. Environ. Pollut. 173, 224–230.

Swarzenski, P.W., Campbell, P.L., Osterman, L.E., Poore, R.Z., 2008. A 1000-year sediment record of recuring hypoxia off the Mississippi River: the potential role of terrestrially-derived organic matter inputs. Mar. Chem. 109, 130–142.

Tarnecki, J.H., Patterson III, W.F., 2015. Changes in red snapper diet and trophic ecology following the Deepwater Horizon oil spill. Marine and Coastal Fisheries: Dynamics, Management, and Ecosystem Science 7, 135–147.

Thomas, C.J., Cahoon, L.B., 1993. Stable isotope analyses differentiate between different trophic pathways supporting rocky-reef fishes. Marine Ecology-Progress Series 95, 19–24.

Todorova, S., Driscoll, C.T., Matthews, D.A., Effler, S.W., 2015. Zooplankon community changes confound the biodilution theory of methylmercury accumulation in a recovering mercury-contaminated Lake. Environmental Science & Technology 49 (7), 4066–4071.

Trefry, J.H., Trocine, R.P., M.L., M., Rember, R.D., Hawkins, L.T., 2007. Total mercury and methylmercury in sediments near offshore drilling sites in the Gulf of Mexico. Environ. Geol. 53, 375–385.

Trudel, M., Rasmussen, J.B., 1997. Modeling the elimination of mercury by fish. Environmental Science & Technology 31 (6), 1716–1722.

Walker, N.D., 1996. Satellite assessment of Mississippi River plume variability: causes and predictability. Remote Sens. Environ. 58, 21–35.

Walsh, J.J., Lenes, J.M., Darrow, B.P., Parks, A.A., Weisberg, R.H., Zheng, L., Hu, C., Barnes, B.B., Daly, K.L., Shin, S.-I., Brooks, G.R., Jeffrey, W.H., Snyder, R.A., Hollander, D., 2015. A simulation analysis of the plankton fate of the *Deepwater Horizon* oil spills. Cont. Shelf Res. 107, 50–68.

Wang, X., Wang, W.-X., 2017. Selenium induces the demethylation of mercury in marine fish. Environ. Pollut. 231, 1543–1551.

Wang, X.-C., Chen, R.F., Gardner, G.B., 2004. Sources and transport of dissolved and particulate organic carbon in the Mississipi River estuary and adjacent coastal waters of the northern Gulf of Mexico. Mar. Chem. 89, 241–256.

Wang, R., Feng, X., Wang, W.-X., 2013. In vivo mercury methylation and demethylation in freshwater tilapia quantified by mercury stable isotopes. Environmental Science & Technology 47 (14), 7949–7957.

Wang, X., Fengchang, W., Wang, W.-X., 2017. In vivo mercury demethylation in a marine fish. Environmental Science & Technology 51 (11), 6441–6451.

Weisberg, R.H., Zheng, L., Liu, Y., Murawski, S., Hu, C., Paul, J., 2016. Did Deepwater Horizon hydrocarbons transit to the west Florida continental shelf? Deep-Sea Research Part II: Topical Studies in Oceanography 129, 259–272.

Wilhelm, S.M., Liang, L., Cussen, D., Kirchgessner, D.A., 2007. Mercury in crude oil processed in the United States. Environmental Science & Technology 41 (13), 4509–4514.

Wise, C.F., Wise, J.T.F., Wise, S.S., Thompson, W.D., Wise Jr., J.P., Wise Sr., J.P., 2014. Chemical dispersants used in the Gulf of Mexico oil crisis are cytotoxic and genotoxic to sperm whale skin cells. Aquat. Toxicol. 152, 335–340.

Wu, P., Kainz, M.J., Bravo, A.G., Akerblom, S., Sonesten, L., Bishop, K., 2019. The importance of bioconcentration into the pelagic food web base for methylmercury biomagnification: a meta-analysis. Sci. Total Environ. 646, 357–367.

Yamashita, M., Yamashita, Y., Suzuki, T., Kani, Y., Mizusawa, N., Imamura, S., Takemoto, K., Hara, T., Hossain, M.A., Yabu, T., Touhata, K., 2013. Selenoneine, a novel selenium-containing compound, mediates detoxification mechanisms against methylmercury accumulation and toxicity in zebrafish embryo. Mar. Biotechnol. 15, 559–570.

Zapp Sluis, M., Boswell, K.M., Chumchal, M.M., Wells, R.J.D., Soulen, B., Cowan Jr., J.H., 2013. Regional variation in mercury and stable isotopes of red snapper (*Lutjanus campechanus*) in the northern Gulf of Mexico, USA. Environ. Toxicol. Chem. 32 (2), 434–441.

Zhang, T., Kim, B., Levard, C., Reinsch, B.C., Lowry, G.V., Deshusses, M.A., Hsu-Kim, H., 2011. Methylation of mercury by bacteria exposed to dissolved, nanoparticulate, and microparticulate mercuric sulfides. Environmental Science & Technology 46 (13), 6950–6958.

Zhu, W., Song, Y., Adediran, G.A., Jiang, T., Reis, A.T., Pereira, E., Skyllberg, U., Bjorn, E., 2018. Mercury transformations in resuspended contaminated sediment controlled by redox conditions, chemical speciation and sources of organic matter. Geochim. Cosmochim. Acta 220, 158–179.

Ziervogel, K., Joye, S., Arnosti, C., 2016. Microbial enzymatic activity and secondary production in sediments affected by the sedimentation pulse following the Deepwater Horizon oil spill. Deep-Sea Research Part II: Topical Studies in Oceanography 129, 241–248.